Nanomed Res J 3(3):154-160, Summer 2018

RESEARCH ARTICLE

Effect of TiO_2 nano-particles on corrosion behavior of Co-Cr alloy coatings in simulated body fluid

Soheil Mahdavi[1]*, Saeid Reza Allahkaram[2], Mohsen Adabi[3]

[1] Research Center for Advanced Materials, Faculty of Materials Engineering, Sahand University of Technology, Tabriz, Iran

[2] School of Metallurgy and Materials Engineering, University College of Engineering, University of Tehran, Tehran, Iran

[3] Young Researchers and Elite Club, Roudehen Branch, Islamic Azad University, Roudehen, Iran

ARTICLE INFO

Article History:
Received 02 April 2018
Accepted 17 June 2018
Published 01 July 2018

Keywords:
Body Fluid
Co-Cr/TiO_2 Coating
Corrosion Behavior
Electrodeposition

ABSTRACT

Co-Cr and Co-Cr/nano-TiO_2 coatings were electrodeposited from Cr(III) based baths. The effect of TiO_2 nano-particles incorporation on the morphology, structure, crystallite size, and preferred orientation was studied. Corrosion behavior of the composite coating was also investigated by means of polarization and electrochemical impedance spectroscopy techniques in Hanks' simulated body fluid, and the results were compared to the unreinforced Co-Cr film. SEM micrographs revealed that the TiO_2 nano-particles have been distributed uniformly within the Co-Cr matrix. Co-deposition of these particles insignificantly changed the nodular morphology of the Co-Cr film. Both the coatings had hcp-Co structure with the highest relative texture coefficient (RTC) for the (100) peak. According to the corrosion results, corrosion potential of the Co-Cr/TiO_2 was nobler than the Co-Cr film and its corrosion current density was about 0.75 of that for the unreinforced alloy coating. The charge transfer resistance of the Co-Cr coating in Hanks' solution was increased from 73.6 to 127.9 kΩ cm^2 by incorporation of TiO_2 nano-particles. However, the double layer capacitance of the Co-Cr film was about 3 times higher than the Co-Cr/TiO_2 coating.

How to cite this article
Mahdavi S, Allahkaram SR, Adabi M. Effect of TiO_2 nano-particles on corrosion behavior of Co-Cr alloy coatings in simulated body fluid. Nanomed Res J, 2018; 3(3): 154-160. DOI: 10.22034/nmrj.2018.03.006

INTRODUCTION

Co-Cr alloys due to outstanding mechanical properties, good biocompatibility, high corrosion and wear resistance are extensively used for the manufacture of prostheses [1,2]. However, metal ions released from Co-Cr alloy in body fluid can cause the toxicity problem [3]. To overcome this obstacle, different surface treatments such as plasma spray, ion implantation and electrodeposition have been developed [4,5]. Among these techniques, electrodeposition is a simple and cost effective method for the preparation of coating on the substrates with different geometries [6-8].

Examination of published literature shows that the optimum wear and corrosion resistance of Co-Cr alloys are usually achieved in presence of 10-30 wt.% chrominum [9]. In recent years, electrodeposition of Cr from hexavalent chromium electrolytes, because of the toxic and genotoxic effects of hexavalent chromium in environment, is substituted by trivalent chromium baths [10]. The preparation of Co-Cr alloys coatings via electrodeposition process from Cr(III) based electrolytes has been reported by Czakonagy *et al.* [11]. They found that an increase in temperature or decrease in current density led to reduction in chromium content of the alloys. Saravanan and Mohan [9] have studied the corrosion resistance of Co-(19-35%)Cr alloys deposited from electrolyte containing $CoCl_2$, and $CrCl_3$ without any Cr complexing agent. They showed that corrosion resistance of Co-35%Cr alloy was better than Co-19%Cr one.

* Corresponding Author Email: *mahdavi@sut.ac.ir*

Electrodeposited composite coatings prepared by dispersion of particles into the metal matrix have better wear and corrosion properties than pure metallic coatings. So far, the incorporation of different particles such as ZrO_2, SiC, Al_2O_3, TiO_2, La_2O_3 and CeO_2 into the metal matrix has been reported [12]. Among these particles, TiO_2 particles have been used as bioactive ceramic for improvement of wear and corrosion resistance due to excellent biocompatibility [13]. Therefore, the distribution of TiO_2 particles in a Co-Cr matrix produced composite coating can give remarkable properties with possibilities to use them as medical prosthetic implant devices. Furthermore, to the author's knowledge, there are few studies regarding the electrodeposition of TiO_2 particles in the Co-Cr matrix. Hence, the purpose of this study is to investigate the morphology, microstructure and corrosion properties of Co-Cr/TiO_2.

EXPERIMENTAL

Co-Cr and Co-Cr/nano-TiO_2 coatings were electrodeposited from Cr(III) based baths using the direct current. The bath composition has been presented in Table 1. Analytical grade chemicals and distilled water were used for preparing the baths. The current densities for electrodeposition of Co-Cr and Co-Cr/TiO_2 coatings were 150 and 140 mA cm^{-2}, respectively. The bath temperature kept constant at 30±1°C during the 30 min of deposition time. The pH was adjusted to 1.5 by using 1M NaOH or 4M H_2SO_4 solution. To achieve to a uniform dispersion of TiO_2 nano-particles and prevent their agglomeration in the bath and within the final coatings, the composite bath was stirred for 24h and ultrasonically treated for 45 min before the electrodeposition process.

The 316L stainless steel plates with an exposed area of 9 cm^2 were used as the substrate. The anode was a same sized dimensionally stable Ti/IrO_2 sheet, which was maintained 3 cm away from the cathode. Prior to the electrodeposition, the substrates were abraded with different grades of emery papers (up to 2000 grit). Degreasing was performed in two steps. First, the substrates were put into acetone in an ultrasonic bath at room temperature for 10 min, and then they were immersed in an alkaline solution (containing NaOH, Na_2CO_3, $Na_2PO_4.12H_2O$) at 70°C for 15 min. Finally, the substrate were pickled in a solution containing hydrochloric acid and cobalt chloride, in accordance with ASTM B254.The substrates were transferred to the electrodeposition bath immediately after activation.

Table 1. The electrodeposition bath composition of Co-Cr and Co-Cr/TiO_2 coatings

Bath composition	Amount
$Cr_2(SO_4)_3.6H_2O$	0.35 M
$CoSO_4.7H_2O$	0.1 M
H_3BO_3	0.9 M
Na_2SO_4	0.6 M
$C_3H_4O_4$ (Malonic acid)	0.6 M
$C_6H_8O_7$ (Citric acid)	0.4 M
$NaC_{12}H_{25}SO_4$ (SDS)	0.2 g L^{-1}
TiO_2 (average size of about 30 nm)	0 and 20 g L^{-1}

Chemical composition and morphology of the alloy and nano-composite coatings were evaluated using a scanning electron microscope equipped with an energy dispersive X-ray spectrometer (EDS). The structure, crystallite size, and preferred orientation of the electrodeposits were analyzed by the X-ray diffraction (XRD) technique. Philips X'Pert Pro XRD apparatus with Cu-K_α beam (λ=1.542 Å) was used for this purpose. The 2-theta range, step size, and time per step were 10-110°, 0.02°, and 0.4 s, respectively. Crystallite size was estimated by using the Williamson-Hall equation. The effect of TiO_2 nano-particles incorporation on preferred orientation was investigated using the relative texture coefficient (Eq. 1) [14-17]:

$$RTC_{hkl} = \frac{I_{hkl}/I^0_{hkl}}{\sum_1^5 I_{hkl}/I^0_{hkl}} \times 100 \quad (1)$$

In this equation, I_{hkl} is the diffraction intensities of the coatings (hkl) lines, and I^0_{hkl} is those for randomly oriented cobalt powder (JCPDS no. 5-0727). Five reflection lines of (002), (100), (110), (101) and (112) for Co were used to calculate the RTC values.

Corrosion behavior of the coatings was studied by potentiodynamic polarization and electrochemical impedance spectroscopy (EIS) in the simulated body fluid (Hanks' solution). The chemical composition of the used Hanks' solution was (in g L^{-1}) 8 NaCl, 0.14 CaCl2, 0.4 KCl, 0.1 MgCl2.6H2O, 0.1 MgSO4.7H2O, 0.35 NaHCO3, 0.12 Na2HPO4.12H2O, 0.06 KH2PO4, and 1 C6H12O6. The tests were performed by using a Bio-Logic SP-300 potentiostat/galvanostat, while the counter and reference electrodes were a platinum sheet (1 cm^2) and an Ag/AgCl (3M KCl),

respectively. The scan rate during the polarization tests was 1 mV s^{-1}. EIS measurements were carried out over a frequency range from 100 kHz to 10 mHz, using a 10 mV amplitude sinusoidal voltage. The obtained data were analyzed by EC-Lab software. For calculating the corrosion rate the Eq. 2 was used [15,18].

$$Corrosion\ rate\ \left(\frac{\mu m}{year}\right) = 315360 \times \frac{\alpha i_{corr}}{nF\rho} \qquad (2)$$

where α is the atomic weight (g mol^{-1}), i_{corr} is the corrosion current density (μA cm^{-2}), n is the number of equivalent exchange, ρ is the density (g cm^{-3}), and F is Faraday's constant (C mol^{-1}).

RESULTS AND DISCUSSION

Chemical composition

According to EDS analysis results, the volume fraction of co-deposited TiO_2 particles is 5.8 vol.%. These particles have been uniformly distributed within the alloy film, as indicated in the SEM micrograph from cross-section of the composite coating in Fig. 1. No agglomeration of nano-particles is also observed in this figure due to the appropriate preparation process of the composite electrodeposition bath. It should be noted that the chromium content of both the Co-Cr and Co-Cr/TiO_2 coatings was about 29 wt.%.

Morphology

Morphology of the Co-Cr and Co-Cr/TiO_2 coatings are shown in Fig. 2. Both the coatings have nodular morphology and contain micro-cracks. However, the density of defects is reduced by incorporation of TiO_2 nano-particles. This can be due to the higher toughness of composite film as compared to the alloy coating, as also reported by other investigators [19-21].

Microstructure

X-ray diffraction patterns of Co-Cr and Co-Cr/TiO_2 coatings are demonstrated in Fig. 3. The structure of the alloy film is not changed by incorporation of TiO_2 nano-particles. The detected peaks are related to the Co with hexagonal close-packed (hcp) structure. Small TiO_2 peaks are also appeared in the XRD pattern of the nano-composite coating. The Cr peaks cannot be observed in these

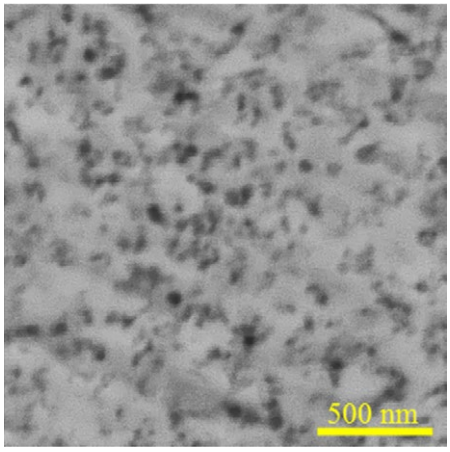

Fig. 1. Backscattered SEM micrograph from cross-section of Co-Cr/5.8vol.%TiO_2 coating.

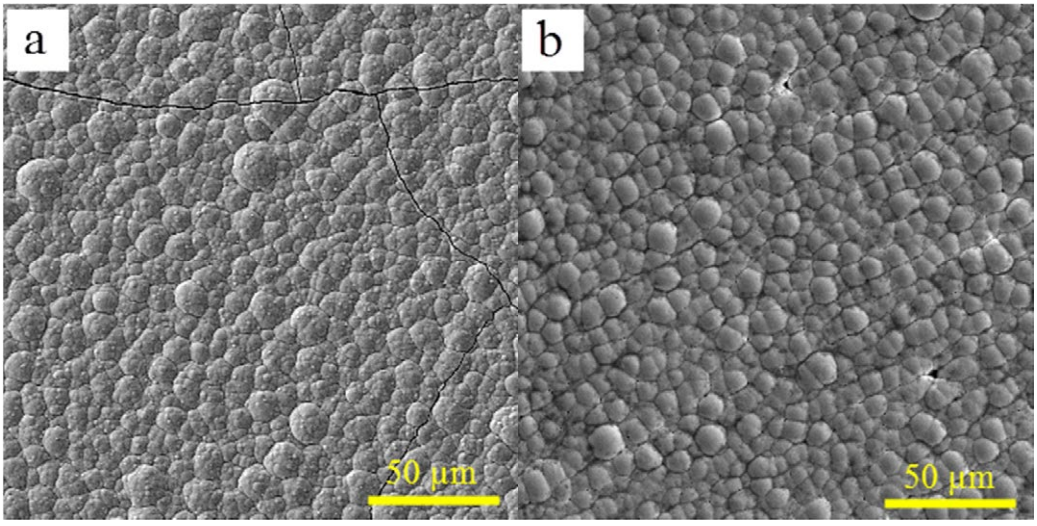

Fig. 2. SEM micrographs from surface of the as-deposited (a) Co-Cr and (b) Co-Cr/TiO_2 coatings.

patterns, which indicates formation of substantial solid solution of Cr in Co.

Crystallite size were calculated by using the Williamson-Hall technique. Incorporation of nano-particles has a negligible effect on the crystallite size of the coatings, and both of these films have nano-crystalline structure. The calculated crystallite size for Co-Cr and Co-Cr/TiO_2 coatings are 10 and 9 nm, respectively.

The relative intensity of diffraction peaks is slightly changed by incorporation of TiO_2 particles. Relative texture coefficient values of five diffraction lines are presented in Table 2. It is observed that $RTC_{(100)}$ has the highest value between all the diffraction lines in both the samples. Therefore, the coatings have [100] texture, and main part of the grains are aligned with their basal plane vertical to the surface of the deposit.

Corrosion behavior

Polarization curves of Co-Cr and Co-Cr/TiO_2 coatings after 1 h immersion in Hanks' solution are shown in Fig. 4. Corroison potentials and corrosion current densities were calculated by Tafel extrapolation technique. Corrosion rates (μm/year) were calculated by using the Eq.2, and the results are presented in Table 3.Corrosion potential shifts to more positive values by incorporation of TiO_2 nano-particles, indicating nobler behavior of composite coating as compared to the Co-Cr film in the simulated body fluid.

Corrosion current density and corrosion rate decrease with co-deposition of nano-particles. Corrosion rate of composite coating is about 22% lower than the Co-Cr film. Higher corrosion resistance of composite coating can be due to two reasons. First, decrement of the metallic surface area in contact with the corrosive media with incorporation of ceramic nano-particles. Second, lower density of defects of composite film than the alloy electrodeposit, as it is clear in Fig. 2.

EIS experiments were also performed for further investigation of corrosion behavior of the coatings in Hanks's solution. The Nyquist plots for Co-Cr and Co-Cr/TiO_2 coatings are shown in Fig. 5. The Nyquist plots of both the coatings show single depressed semi-circles, representing the presence of one capacitive time constant and deviation from ideal dielectric behavior because of the surface heterogeneities [15,22-25]. The presence of one

Table 2. Relative texture coefficient values for different diffraction lines

Sample	$RTC_{(100)}$	$RTC_{(002)}$	$RTC_{(101)}$	$RTC_{(110)}$	$RTC_{(112)}$
Co-Cr	42.4	29.2	10.4	10.0	8.1
Co-Cr/TiO_2	41.3	40.2	8.8	5.2	4.5

Table 3. Electrochemical parameters obtained from polarization curves

Sample	E_{corr} (mV)	i_{corr} (μA cm^{-2})	β_a (mV/decade)	β_c (mV/decade)	Corrosion rate (μm/year)
Co-Cr	-360	0.055	97	82	0.41
Co-Cr/TiO_2	-300	0.042	108	85	0.32

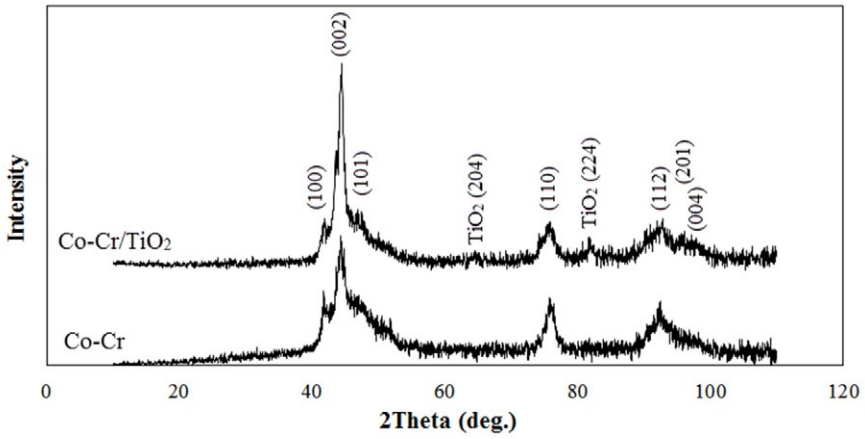

Fig. 3. XRD patterns of Co-Cr and Co-Cr/TiO_2 coatings.

capacitive time constant is also confirmed by Bode plots in Fig. 6. Therefore, as shown in Fig. 5, a simple Randles equivalent circuit is used to fit the experimental data of the both samples. In this circuit, R_s is the solution resistance between the working and the reference electrode, R_p is the charge transfer resistance, and CPE (constant phase element) is capacitance of the coatings. The calculated electrochemical parameters are presented in Table 4. EIS results are in good agreement with polarization data. Charge-transfer resistance of the Co-Cr/TiO_2 coating is about 1.7 times higher than the Co-Cr film, which means that it has better corrosion resistance than the alloy sample in the simulated body fluid.

It is also clear from Table 4 that the Co-Cr film has higher double layer capacitance than the composite coating. The double layer capacitance is directly related to the surface area involved in the electrochemical reactions [26]. The presence of open voids and cracks can increase this surface area and cause to higher capacitance. As the density of defects is decreased by co-deposition of nano-TiO_2 particles, the composite coating has lower double

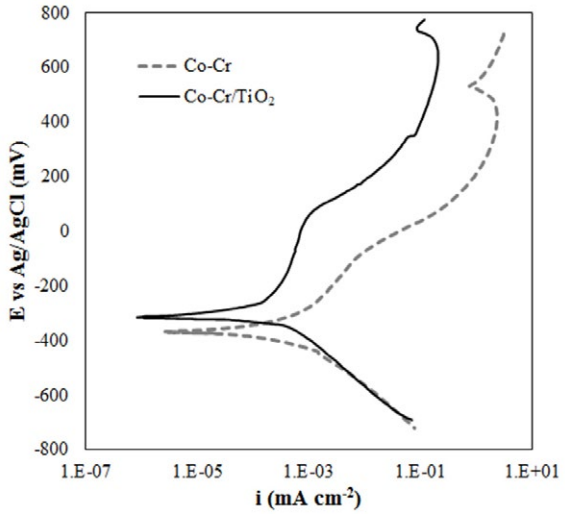

Fig. 4. Polarization curves of Co-Cr and Co-Cr/TiO_2 coatings after 1 h immersion in simulated body fluid.

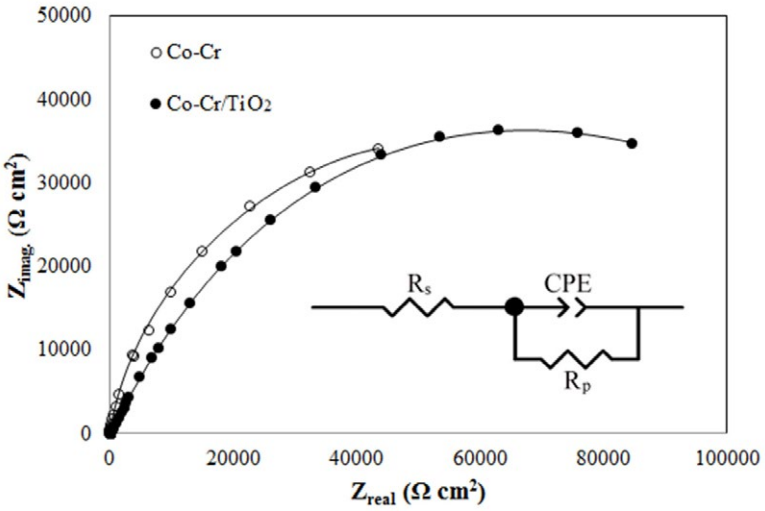

Fig. 5. Nyquist plots of Co-Cr and Co-Cr/TiO_2 and the equivalent circuit used to fit the experimental data.

Table 4. The equivalent circuit parameters of Co-Cr and Co-Cr/TiO_2 coatings after 1 h immersion in Hanks' solution

Sample	R_s (Ω cm^2)	R_p (kΩ cm^2)	C (μF cm^{-2})
Co-Cr	27.5	73.6	549.7
Co-Cr/TiO_2	81.7	127.9	177.0

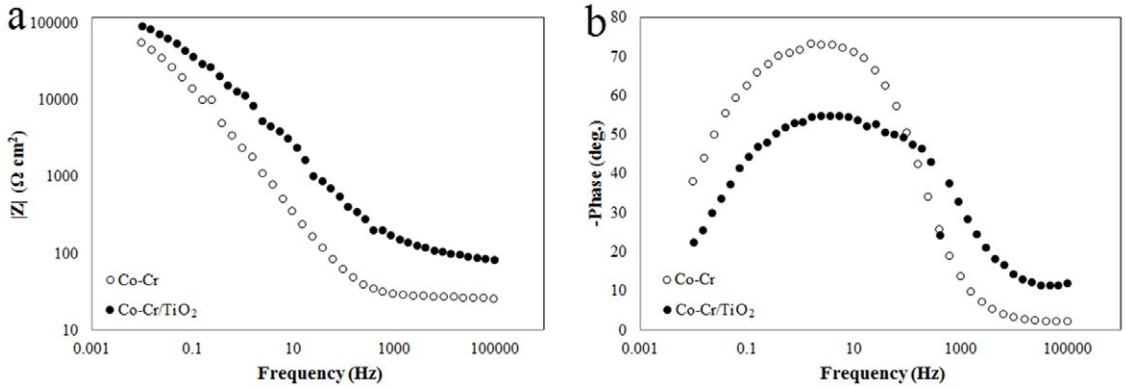

Fig. 6. Bode plots of electrodeposited Co-Cr and Co-Cr/TiO_2 coatings.

layer capacitance than the alloy film. Another reason can be decrement of metallic surface in contact with corrosive media in presence of the ceramic particles.

CONCLUSIONS

In this study, Co-Cr alloy and Co-Cr/TiO_2 nano-composite coatings were produced by electrodeposition technique. The effect of TiO_2 nano-particles incorporation on morphology, structure, and corrosion behavior of Co-Cr alloy film in simulated body fluid was investigated. The outcome of the results can be summarized as follows:

1- The amount of co-deposited TiO_2 nano-particles was 5.8 vol.%, which were uniformly dispersed within the Co-Cr matrix. Both the alloy and composite coatings contained about 29 wt.% Cr.

2- Nodular morophology of the Co-Cr film was not changed by incorporation of nano-particles. However, the density of defects of the Co-Cr/TiO_2 coating was lower than the unreinforced one.

3- Both the coatings were nano-crystalline substantial solid solution of Cr in Co with hcp structure, and [100] texture.

4- Corrosion potential shifted to more positive values and corrosion rate about 22% decreased with incorporation of TiO_2 nano-particles.

5- According to EIS results, charge transfer resistance of Co-Cr/TiO_2 coatings was about 1.7 time of that for Co-Cr film in the simulated body fluid (Hanks' solution), indicating better corrosion resistance of the composite coating.

CONFLICT OF INTEREST

The authors declare that there are no conflicts of interest regarding the publication of this manuscript.

REFERENCES

1. Placko HE, Brown SA, Payer JH. Effects of microstructure on the corrosion behavior of CoCr porous coatings on orthopedic implants. Journal of Biomedical Materials Research. 1998;39(2):292-9.
2. Nielsen K. Corrosion of metallic implants. British Corrosion Journal. 1987;22(4):272-8.
3. Ng BS, Annergren I, Soutar AM, Khor KA, Jarfors AEW. Characterisation of a duplex TiO2/CaP coating on Ti6Al4V for hard tissue replacement. Biomaterials. 2005;26(10):1087-95.
4. Zhao X, Liu X, Ding C, Chu PK. In vitro bioactivity of plasma-sprayed TiO2 coating after sodium hydroxide treatment. Surface and Coatings Technology. 2006;200(18-19):5487-92.
5. Paital SR, Dahotre NB. Calcium phosphate coatings for bio-implant applications: Materials, performance factors, and methodologies. Materials Science and Engineering: R: Reports. 2009;66(1-3):1-70.
6. Adabi M, Amadeh A. Effect of electrodeposition conditions on properties of Ni–Al composite coatings. Surface Engineering. 2015;31(9):650-8.
7. Adabi M, Amadeh AA. Electrodeposition mechanism of Ni–Al composite coating. Transactions of Nonferrous Metals Society of China. 2014;24(10):3189-95.
8. M. Adabi, A. Amadeh, Improvement of adhesion, corrosion

and wear resistance of Ni electrodeposited coating by applying Cu intermediate layer after zincate process, Indian Journal of Engineering & Materials Sciences, 24 (2017), 306-312.
9. Saravanan G, Mohan S. Structure, composition and corrosion resistance studies of Co–Cr alloy electrodeposited from deep eutectic solvent (DES). Journal of Alloys and Compounds. 2012;522:162-6.
10. Choi Y-I, Eguchi T, Asao T, Kuroda K, Okido M. Mechanism for the Formation of Black Cr-Co Electrodeposits from Cr3+Solution Containing Oxalic Acid. Journal of The Electrochemical Society. 2014;161(14):D713-D8.
11. Czakó-Nagy I, El-Sharif MK, Vértes A, Chisholm CU. Studies of electrodeposited chronium-cobalt alloy coatings by emission Co-57 Mössbauer spectroscopy. Electrochimica Acta. 1994;39(6):801-5.
12. Benea L, Ponthiaux P, Wenger F. Co-ZrO2 electrodeposited composite coatings exhibiting improved micro hardness and corrosion behavior in simulating body fluid solution. Surface and Coatings Technology. 2011;205(23-24):5379-86.
13. Mahdavi S, Allahkaram SR. Composition, characteristics and tribological behavior of Cr, Co–Cr and Co–Cr/TiO 2 nano-composite coatings electrodeposited from trivalent chromium based baths. Journal of Alloys and Compounds. 2015;635:150-7.
14. Spanou S, Pavlatou EA, Spyrellis N. Ni/nano-TiO2 composite electrodeposits: Textural and structural modifications. Electrochimica Acta. 2009;54(9):2547-55.
15. Ebrahim-Ghajari M, Allahkaram SR, Mahdavi S. Corrosion behaviour of electrodeposited nanocrystalline Co and Co/ZrO2nanocomposite coatings. Surface Engineering. 2014;31(3):251-7.
16. Lajevardi SA, Shahrabi T. Effects of pulse electrodeposition parameters on the properties of Ni–TiO2 nanocomposite coatings. Applied Surface Science. 2010;256(22):6775-81.
17. Mahdavi S, Allahkaram SR. Characteristics of electrodeposited cobalt and titania nano-reinforced cobalt composite coatings. Surface and Coatings Technology. 2013;232:198-203.
18. Karimi S, Nickchi T, Alfantazi A. Effects of bovine serum albumin on the corrosion behaviour of AISI 316L, Co–28Cr–6Mo, and Ti–6Al–4V alloys in phosphate buffered saline solutions. Corrosion Science. 2011;53(10):3262-72.
19. liu B, Zeng Z, Lin Y. Mechanical properties of hard Cr–MWNT composite coatings. Surface and Coatings Technology. 2009;203(23):3610-3.
20. Surviliene S, Jasulaitiene V, Lisowska-Oleksiak A, Safonov VA. Effect of WC on electrodeposition and corrosion behaviour of chromium coatings. Journal of Applied Electrochemistry. 2005;35(1):9-15.
21. Gao J, Suo J. Preparation and characterization of the electrodeposited Cr–Al2O3/SiC composite coating. Applied Surface Science. 2011;257(22):9643-8.
22. Ciubotariu AC, Benea L, Lakatos–Varsanyi M, Dragan V. Electrochemical impedance spectroscopy and corrosion behaviour of Al2O3–Ni nano composite coatings. Electrochimica Acta. 2008;53(13):4557-63.
23. Aruna ST, Ezhil Selvi V, William Grips VK, Rajam KS. Corrosion- and wear-resistant properties of Ni–Al2O3 composite coatings containing various forms of alumina. Journal of Applied Electrochemistry. 2011;41(4):461-8.
24. Ranjith B, Paruthimal Kalaignan G. Ni–Co–TiO2 nanocomposite coating prepared by pulse and pulse reversal methods using acetate bath. Applied Surface Science. 2010;257(1):42-7.
25. Lebrini M, Fontaine G, Gengembre L, Traisnel M, Lerasle O, Genet N. Corrosion behaviour of galvanized steel and electroplating steel in aqueous solution: AC impedance study and XPS. Applied Surface Science. 2008;254(21):6943-7.
26. Rosalbino F, Scavino G, Mortarino G, Angelini E, Lunazzi G. EIS study on the corrosion performance of a Cr(III)-based conversion coating on zinc galvanized steel for the automotive industry. Journal of Solid State Electrochemistry. 2010;15(4):703-9.